Inorg. Chem. **2006**, *45*, 6298–6307

Molecular and Electronic Structures of Tetrahedral Complexes of Nickel and Cobalt Containing *N,N′*-Disubstituted, Bulky *o*-Diiminobenzosemiquinonate(1–) π-Radical Ligands

Krzysztof Chłopek, Eberhard Bothe, Frank Neese, Thomas Weyhermüller, and Karl Wieghardt*

Max-Planck-Institut für Bioanorganische Chemie, Stiftstrasse 34-36, D-45470 Mülheim an der Ruhr, Germany

Received February 13, 2006

The reaction of 2 equiv of the bulky ligand *N,N′*-bis(3,5-di-*tert*-butylphenyl)-1,2-phenylenediamine, $H_2[^3L^{PDI}]$, excess triethylamine, and 1 equiv of $M(CH_3CO_2)_2{\cdot}4H_2O$ (M = Ni, Co) in the presence of air in CH_3CN/CH_2Cl_2 solution yields violet-black crystals of $[Ni^{II}(^3L^{ISQ})_2]$ CH_3CN (**1**) or violet crystals of $[Co(^3L)_2]$ (**3**). By using $Pd(CH_3CO_2)_2$ as starting material, green-blue crystals of $[Pd^{II}(^3L^{ISQ})_2]{\cdot}CH_3CN$ (**2**) were obtained. Single-crystal X-ray crystallography revealed that **1** and **3** contain (pseudo)tetrahedral neutral molecules $[M(^3L)_2]$ (M = Ni, Co) whereas in **2** nearly square planar, neutral molecules $[Pd^{II}(^3L^{ISQ})_2]$ are present. Temperature-dependent susceptibility measurements established that **1** and **2** are diamagnetic ($S = 0$) whereas **3** is paramagnetic with an $S = {}^3/_2$ ground state. It is shown that **1** contains two π radical benzosemiquinonate(1–)-type monoanions, $((^3L^{ISQ})^{1-\bullet}$, $S_{rad} = {}^1/_2)$, and a central Ni(II) ion (d^8; $S = 1$) which are antiferromagnetically coupled yielding the observed $S_t = 0$ ground state. This result has been confirmed by broken symmetry DFT calculations of **1**. In contrast, the $S_t = {}^3/_2$ ground state of **3** is more difficult to understand: the two resonance structures $[Co^{III}(^3L^{ISQ})(^3L^{PDI})] \leftrightarrow [Co^{II}(^3L^{PDI})(^3L^{IBQ})]$ might be invoked (for tetrahedral $[Co^{II}(^3L^{ISQ})_2]$ containing an $S_{Co} = {}^3/_2$ with two antiferromagnetically coupled π-radical ligands an $S_t = {}^1/_2$ is anticipated). Complex **2** is diamagnetic ($S = 0$) containing a Pd^{II} ion (d^8, $S_{Pd} = 0$ in an almost square planar ligand field) and two antiferromagnetically coupled ligand radicals ($S_{rad} = {}^1/_2$). The electrochemistry and spectroelectrochemistry of **1, 2**, and **3** have been studied, and electron-transfer series comprising the species $[M(L)_2]^z$ ($z = 2+, 1+, 0, 1-, 2-$) have been established. All oxidations and reductions are ligand centered.

Introduction

The reaction of *o*-phenylenediamine, $H_2[^1L^{PDI}]$, with MX_2 salts (ratio 2:1) (M = Ni, Pd, Pt) affords in the presence of air dark blue/black microcrystals of neutral, square planar, and diamagnetic complexes $[M(^1L^{ISQ})_2]$, where $(L^{ISQ})^{1-\bullet}$ represents the *o*-diiminobenzosemiquinonate π-radical monoanion (Figure 1).

These species have been shown to be the central member of an electron-transfer series of five square planar bis(chelate)metal complexes of the type $[MN_4]^z$ with $z = 2-$, $1-$, 0, $1+$, $2+$ which are interrelated by four reversible one-electron-transfer steps.[1] These have been elucidated to be ligand-centered processes where each ligand may adopt an oxidation level as *o*-phenylenediimide(2−), $(L^{PDI})^{2-}$, *o*-diiminobenzosemiquinonate(1−), $(L^{ISQ})^{1-\bullet}$, or *o*-diiminebenzoquinone, $(L^{IBQ})^0$. The corresponding series has also been reported[1] for $[Co(^1L)_2]^0$, which itself possesses an $S = {}^1/_2$ ground state. All of these species containing unsubstituted *o*-phenylenediamine-type ligands are square planar.

We and others have recently shown[2] that the corresponding square planar complexes $[M(^2L)_2]$ (M = Ni, Pd, Pt) containing two *N*-phenyl-*o*-phenylenediamine, $[^2L^{PDI}]H_2$, derived ligands also exist and that they also form five-membered electron-transfer series. The corresponding complex $[Co(^2L)_2]$ ($S = {}^1/_2$) is again square planar.[3] From experimental data and DFT, as well as ab initio, calculations, it has been elucidated that the electronic structure of this latter species

* To whom correspondence should be addressed. E-mail: wieghardt@mpi-muelheim.mpg.de. Phone: ++49-208-306 3610. Fax: ++49-208-306 3952. .

(1) Balch, A. L.; Holm, R. H. *J. Am. Chem. Soc.* **1966**, *88*, 5201.

(2) (a) Herebian, D.; Bothe, E.; Neese, F.; Weyhermüller, T.; Wieghardt, K. *J. Am. Chem. Soc.* **2003**, *125*, 9116. (b) Herebian, D.; Wieghardt, K. E.; Neese, F. *J. Am. Chem. Soc.* **2003**, *125*, 10997.

(3) Bill, E.; Bothe, E.; Chaudhuri, P.; Chlopek, K.; Herebian, D.; Kokatam, S.; Ray, K.; Weyhermüller, T.; Neese, F.; Wieghardt, K. *Chem. Eur. J.* **2005**, *11*, 204.

10.1021/ic060242l CCC: $33.50
Published on Web 07/15/2006

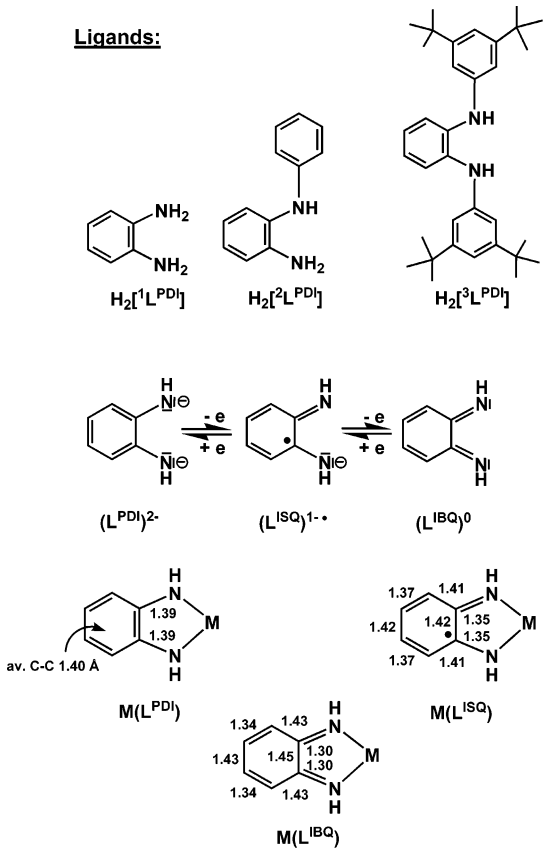

Figure 1. Ligands and abbreviations used in this work. PDI = *o*-phenylenediimide(2−), ISQ = *o*-diiminobenzosemiquinonate(1−), IBQ = *o*-diiminobenzoquinone. Bond distances are given in Å for the M(L^{IBQ}), M(L^{ISQ}), and M(L^{PDI}) fragments. They were obtained from X-ray crystallographic structure determinations (refs 2, 3).

Scheme 1

Complexes:

$[Ni^{II}(^3L^{ISQ})_2]\cdot CH_3CN$	(**1**)	tetrahedral	S = 0
$[Pd^{II}(^3L^{ISQ})_2]\cdot CH_3CN$	(**2**)	square planar	S = 0
$[Co(^3L)_2]$	(**3**)	tetrahedral	S = 3/2

may be described as $[Co^{II}(^2L^{ISQ})_2]$ but the assignment of a Co(II) oxidation state remained somewhat ambiguous;[3] $[Co^{III}(^2L^{PDI})(^2L^{ISQ})]$ is also a possibility where the central cobalt(III) ion (d^6) possesses an intrinsic $S_{Co} = 1$ state which couples antiferromagnetically to a ligand π-radical yielding the observed $S_t = {}^1/_2$ ground state for this molecule. Since both ligands are equivalent, the mixed valency of the ligands is probably best described as class III (delocalized).

Here we report the synthesis of $[Ni(^3L^{ISQ})_2]$ (**1**), $[Pd(^3L^{ISQ})_2]$ (**2**), and $[Co(^3L)_2]$ (**3**) (Scheme 1) where $(^3L)^n$ represents the *o*-phenylenediimide ($n = 2-$), the corresponding radical ($n = 1-$), and the diimine ($n = 0$) derivative of the bulky ligand *N*,*N*′-bis(3,5-di-*tert*-butylphenyl)-1,2-phenylenediamine, $H_2[^3L^{PDI}]$ (Figure 1). Interestingly, **1** and **3** are *tetrahedral* complexes whereas **2** is almost square planar. The electronic structures of these species reveal diamagnetic ground states for **1** and **2**, as has been determined by proton NMR, whereas **3** is paramagnetic ($S_t = {}^3/_2$). The electro- and spectroelectrochemistry of the tetrahedral complexes **1** and **3** are compared with those of nearly square planar **2**. In addition, the electronic structure of tetrahedral **1** has been elucidated by broken symmetry (BS) DFT calculations.

Experimental Section

The ligand *N*,*N*-bis(3,5-di-*tert*-butylphenyl)-1,2-phenylenediamine, $H_2[^3L^{PDI}]$, has been prepared according to a published procedure.[4] A dark brown oil obtained similarly to method described in ref 4c was immediately purified by flash chromatography on silica (gradient elution with *n*-heptane/CH_2Cl_2 (7:0 up to 7:2 v/v, respectively); the silica gel (Merck) contained particles 0.015−0.040 mm and 0.063−0.200 mm mixed in a 2:1 ratio). This procedure affords upon evaporation of the first fraction colorless, oily 2-bromo,1-{*N*-[3,5-di(*tert*-butyl)phenyl]}benzene ($R_f = 0.49$ in *n*-heptane/CH_2Cl_2 7:1 v/v). Evaporation of the second fraction gives the desired product $H_2[^3L^{PDI}]$ as a white solid ($R_f = 0.16$ in *n*-heptane/CH_2Cl_2 7:1 v/v). The latter is contaminated up to 8% with *N*-phenyl-*N*-[3,5-di(*tert*-butyl)phenyl]amine, which can be removed by washing the solid $H_2[^3L^{PDI}]$ with MeCN. Anal. Calcd for $C_{34}H_{48}N_2$: C 84.24, H 9.98, N 5.78; found: C 84.2**,** H 9.9**,** N 5.6. Mass spectrum (EI): $m/z = 484$ $\{M\}^+$. IR (KBr, cm^{-1}), selected peaks: 3374, 3338 ν(NH); 2961, 2901, 2864 ν(CH). ^{1}H NMR (300 K, CD_2Cl_2, 400 MHz): $\delta = 1.29$ (s, *tert*-butyl, 18H); 5.67 (s, NH, 1H); 6.83 (d, 2H, $J = 1.67$ Hz); 6.96 (dd, 1H, $J_1 = 3.49$ Hz, $J_2 = 2.47$ Hz); 6.99 (t, 1H, $J = 1.67$ Hz); 7.27 (dd, 1H, $J_1 = 3.56$ Hz, $J_2 = 2.31$ Hz,). ^{13}C NMR (300 K, CD_2Cl_2, 100 MHz): $\delta = 31.15$, 34.74, 111.91, 114.94, 119.53, 122.35, 135.22, 143.12, 151.93.

The precursor 3,5-di-*tert*-butylaniline was synthesized according to ref 5.

$[Ni^{II}(^3L^{ISQ})_2]\cdot CH_3CN$ (1). To a solution of the ligand $H_2[^3L^{PDI}]$ (0.10 g; 0.21 mmol) in a mixture of acetonitrile (5 mL) and CH_2Cl_2 (3 mL) was added triethylamine (0.5 mL) and $Ni(CH_3CO_2)_2\cdot 4H_2O$ (50 mg; 0.2 mmol). The solution was stirred for 3 days in the presence of air until a dark violet solution was obtained. Then a second equivalent of the ligand was introduced (0.10 g, 0.21 mmol) and the mixture was stirred for additional 5 h, during which time a dark violet-black microcrystalline precipitate formed, which was filtered off, washed with acetonitrile (5 mL), and air-dried. Yield: 92 mg (43%). X-ray-quality single crystals of **1** were grown from a 1:1 mixture of CH_3CN/CH_2Cl_2 (v/v). Anal. Calcd for $C_{68}H_{92}N_4Ni$: C, 79.74; H, 9.05; N, 5.47; Ni, 5.73. Found: C, 79.6; H, 8.9; N, 5.7; Ni, 5.7. Mass spectrum (EI): $m/z = 1022$ $\{M\}^+$. ^{1}H NMR (300 K, CD_2Cl_2, 400 MHz): $\delta = 1.20$ (s, *tert*-butyl, 18H), 7.29 (dd, 1H, $J_1 = 3.23$ Hz, $J_2 = 3.56$ Hz); 7.50 (t, 1H, $J = 1.49$ Hz); 8.00 (dd, 1H, $J_1 = 3.24$ Hz, $J_2 = 3.61$ Hz); 8.13 (d, 2H, $J = 1.59$ Hz). ^{13}C NMR (300 K, CD_2Cl_2, 100 MHz): $\delta = 31.76$, 34.90, 117.3, 117.81, 120.82, 148.42, 153.09, 161.13.

$[Pd^{II}(^3L^{ISQ})_2]\cdot CH_3CN$ (2). A solution of the ligand $H_2[^3L^{PDI}]$ (0.18 g; 0.37 mmol), $Pd(CH_3CO_2)_2$ (42 mg; 0.18 mmol), and NEt_3 (0.5 mL) in CH_2Cl_2 (6 mL) was stirred at 20 °C for 72 h in the presence of air. During this time, the color of the solution changed from brown to dark blue. After addition of acetonitrile (20 mL), the precipitation of microcrystalline **2** was initiated. After filtration, a green-blue microcrystalline powder was obtained. Yield: 77 mg

(4) (a) Alcazar-Roman, L. M.; Hartwig, J. F.; Rheingold, A. L.; Liable-Sands, L. M.; Guzei, I. A. *J. Am. Chem. Soc.* **2000**, *122*, 4618. (b) Hartwig, J. F. *Angew. Chem., Int. Ed. Engl.* **1998**, *37*, 2047. (c) Rivas, F. M.; Riaz, U.; Diver, S. T. *Tetrahedron: Asymmetry* **2000**, *11*, 1703. (d) Wolfe, J. P.; Buchwald, S. L. *Org. Chem.* **2000**, *65*, 1144. (e) Yang, B. H.; Buchwald, S. L. *J. Organomet. Chem.* **1999**, *576*, 125.
(5) (a) Burgers, J.; van Hartingsveldt, W.; van Keulen, J.; Verkade, P. E.; Visser, H.; Wepster, B. M. *Recl. Trav. Chim. Pays-Bas* **1956**, *75*, 1317. (b) Ram, S.; Ehrenkäufer, R. E. *Tetrahedron Lett.* **1984**, *25*, 3415.

Table 1. Crystallographic Data for **1**·MeCN and **3**

	1·MeCN	**3**
chem. formula	$C_{70}H_{95}N_5Ni$	$C_{68}H_{92}CoN_4$
fw	1065.22	1024.39
space group	$P2_1/c$, No. 14	$I4/a$, No.88
a, Å	24.3092(8)	20.357(2)
b, Å	15.1637(5)	20.357(2)
c, Å	18.5850(6)	14.742(2)
α, deg	90	90
β, deg	109.59(1)	90
γ, deg	90	90
V, Å	6454.2(4)	6109.2(12)
Z	4	4
T, K	100(2)	203(2)
ρ_{calcd}, g cm^{-3}	1.096	1.114
reflns collected/$2\theta_{max}$	113 899/50.00	7953/91.21
unique reflns/$I > 2\sigma(I)$	11 290/9222	1269/1189
no. of params/restraints	720/31	185/132
λ, Å/μ(Kα), cm^{-1}	0.71073/3.43	1.54178/25.05
R1[a]/GOF[b]	0.0579/1.106	0.0769/1.243
wR2[c]($I > 2\sigma(I)$)	0.1051	0.1432
residual density, e Å^{-3}	+0.48/−0.46	+0.23/−0.22

[a] Observation criterion: $I > 2\sigma(I)$. $R1 = \sum||F_o| - |F_c||/\sum|F_o|$. [b] $GOF = [\sum[w(F_o^2 - F_c^2)^2]/(n - p)]^{1/2}$. [c] $wR2 = [\sum[w(F_o^2 - F_c^2)^2]/\sum[w(F_o^2)^2]]^{1/2}$ where $w = 1/\sigma^2(F_o^2) + (aP)^2 + bP$, $P = (F_o^2 + 2F_c^2)/3$.

(39%). Anal. Calcd for $C_{68}H_{92}N_4Pd$: C, 76.19; H, 8.65; N, 5.23. Found: C, 76.0; H, 8.6; N, 5.2. Mass spectrum (EI): $m/z = 1070$ $\{M\}^+$. ^{1}H NMR (300 K, CD_2Cl_2, 400 MHz): $\delta = 1.27$ (s, *tert*-butyl, 18H), 6.44 (m, 1H), 6.47 (m, 1H), 7.03 (d, 2H, $J = 1.58$ Hz), 7.09 (t, 1H, $J = 1.66$ Hz). ^{13}C NMR (300 K, CD_2Cl_2, 100 MHz): $\delta = 31.84$, 35.06, 116.11, 119.01, 122.81, 122.96, 148.93, 149.26, 156.98.

[Co(^{3}L)$_2$] (3). To a solution of the ligand $H_2[^3L^{PDI}]$ (0.18 g; 0.38 mmol) in a mixture of CH_3CN (4 mL) and CH_2Cl_2 (5 mL) was added NEt_3 (0.5 mL and $Co(CH_3CO_2)_2 \cdot 4H_2O$ (45 mg; 0.18 mmol). The mixture was stirred in the presence of air at ambient temperature for 1 h, whereupon the color changed to dark violet. The volume of the reaction mixture was reduced to 3 mL by slow evaporation within 5 days. Violet crystals grew slowly which were filtered off, washed with CH_3CN (6 mL), and air-dried. Yield: 0.18 g (96%). Anal. Calcd for $C_{68}H_{92}N_4Co$: C, 79.73; H, 9.05; N, 5.47; Co, 5.75. Found: C, 79.6; H, 9.0; N, 5.4; Co, 5.8. Mass spectrum (EI): $m/z = 1024$ $\{M\}^+$.

X-ray Crystallographic Data Collection and Refinement of the Structures. Black single crystals of **1**·MeCN and **3** were coated with perfluoropolyether, picked up with a glass fiber, and immediately mounted in the nitrogen cold stream of the diffractometer to prevent loss of solvent. A Nonius Kappa-CCD diffractometer equipped with a Mo-target rotating-anode X-ray source and a graphite monochromator (Mo Kα, $\lambda = 0.71073$ Å) was used for **1**. A multiscan absorption correction was applied to the data set. Compound **3** was measured on a Bruker SMART diffractometer with copper radiation (Cu Kα, $\lambda = 1.54178$ Å) from a sealed-tube source and corrected for absorption by SADABS.[6] Final cell constants were obtained from least-squares fits of all measured reflections. The Siemens ShelXTL[7] software package was used for solution and artwork of the structure; ShelXL97[8] was used for the refinement. The structures were readily solved by direct and Patterson methods and subsequent difference Fourier techniques. Crystallographic data of the compounds are listed in Table 1. All non-hydrogen atoms in **1** and **3** were refined anisotropically. Hydrogen atoms attached to carbon atoms were placed at calculated positions and refined as riding atoms with isotropic displacement parameters. The *tert*-butyl groups in **3** were found to be disordered, and two split positions were refined for the methyl carbon atoms C(12)−C(14) and C(16)−C(18). Disorder was also observed for a *tert*-butyl group in **1**. Carbon atoms C(61)−C(64) were split on two positions. Bonded and nonbonded C−C distances were restrained to be equal within errors in both cases (SADI instruction), and equal thermal displacement parameters were given for split atoms (EADP instruction). A second data set of a different crystal of **3** was measured with Mo Kα-radiation at 100 K, but surprisingly, the quality of the structure did not improve.

The thermal displacement parameters are still quite large. Refinement using a split atom model and refinement in the nonisomorphic subgroup $C2/c$ was attempted but did not improve the structure analysis. This suggests that both ligands in **3** are not equivalent and that the structure is statically disordered.

Calculations. All calculations were performed by using the ORCA program package.[9] The geometry optimizations were carried out at the B3LYP level[10] of DFT. The all-electron Gaussian basis sets were those reported by the Ahlrichs group.[11] Triple-ζ-quality basis sets with one set of polarization functions on the nickel and nitrogen atoms were used (TZVP).[11b] The carbon and hydrogen atoms were described by slightly smaller polarized split-valence SV(P) basis sets, that is, double-ζ quality in the valence region and contains a polarizing set of d-functions on the non-hydrogen atoms.[11a] The SCF calculations were tightly converged (1×10^{-8} Eh in energy, 1×10^{-7} Eh in the density change, and 1×10^{-7} in the maximum element of the DIIS error vector). The geometries were considered converged after the energy change was less than 5×10^{-6} Eh, the gradient norm and maximum gradient element were smaller than 1×10^{-4} and 3×10^{-4} Eh/Bohr, respectively, and the root-mean square and maximum displacements of atoms were smaller than 2×10^{-3} and 4×10^{-3} Bohr, respectively.

Physical Measurements. Electronic spectra of complexes and corresponding spectra from electrochemical measurements were recorded on a HP 8452A diode array spectrophotometer (for the range 200−1000 nm) or a Perkin-Elmer double-beam photometer (for the range 200−2000 nm). Cyclic voltammograms and coulometric experiments were performed with an EG&G potentiostat/galvanostat, Model 273A. Variable-field (1−7 T), variable-temperature (4−300 K) magnetization data were recorded on a SQUID magnetometer (MPMS Quantum Design). The experimental magnetic susceptibility data were corrected for underlying diamagnetism by use of tabulated Pascal's constants. X-band EPR spectra were recorded on a Bruker ESP 300 spectrometer.

Results and Discussion

1. Syntheses. The reaction of the ligand *N*,*N*′-bis(3,5-di-*tert*-butylphenyl)-1,2-phenylenediamine, $H_2[^3L^{PDI}]$, with the bis(acetato)metal salts of Ni(II), Pd(II), and Co(II) in the ratio 2:1 in an acetonitrile/dichloromethane solvent mixture in the

(6) *SADABS*, Version 2004-1; Bruker Nonius: Delft, The Netherlands.
(7) *ShelXTL*, Version 5; Siemens Analytical X-ray Instruments, Inc.: Madison, WI, 1994.
(8) Sheldrick, G. M. *ShelXL97*; Universität Göttingen: Göttingen, Germany, 1997.
(9) Neese, F. *ORCA, an Ab Initio, Density Functional and Semiempirical Electronic Structure Program Package*, Version 2.4, Revision 36; Max-Planck-Institut für Bioanorganische Chemie: Mülheim/Ruhr, Germany, May 2005.
(10) (a) Becke, A. D. *J. Chem. Phys.* **1986**, *84*, 4524. (b) Lee, C.; Yang, W.; Parr, R. G. *Phys. Rev. B* **1988**, *37*, 785. (c) Becke, A. D. *J. Chem. Phys.* **1993**, *98*, 5648.
(11) (a) Schäfer, A.; Horn, H.; Ahlrichs, R. *J. Chem. Phys.* **1992**, *97*, 2571. (b) Schäfer, A.; Huber, C.; Ahlrichs, R. *J. Chem. Phys.* **1994**, *100*, 5829.

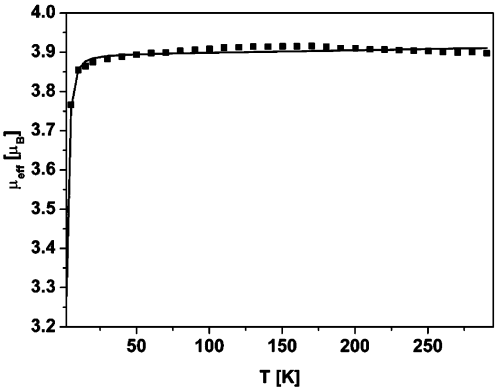

Figure 2. Temperature dependence of the magnetic moment, μ_{eff}, of solid **3**. Filled squares are experimental data, and the solid line represents a fit ($S = {}^3/_2$; $g = 2.01(1)$; $|D| = 2.3(6)$ cm^{-1}, $E/D = 0$, temperature-independent paramagnetism 60(40) $\times$ 10^{-6} emu).

presence of air and excess triethylamine produced deep blue-black solutions from which microcrystals of violet-black **1**, green-blue **2**, and violet **3**, respectively, were obtained.

^{1}H NMR and temperature-dependent (3−300 K) magnetic susceptibility measurements showed that **1** and **2** possess a diamagnetic ground state ($S = 0$). In contrast, as shown in Figure 2, complex **3** is paramagnetic with a temperature-independent magnetic moment of 3.9 μ_B (50−300 K) indicating an $S = {}^3/_2$ ground state.

2. Crystal Structures. The crystal structures of **1** and **3** have been determined by X-ray crystallography; the first at 100(2) K and the latter at 200 K. The structure of **2** has also been determined at 100 K, but the quality of the crystals was low. Due to the large residual *R* factor of ∼18%, we refrain from a detailed discussion of the structure.[12] Table 1 gives the crystallographic data, and Table 2 summarizes important bond lengths in **1** and **3**.

The oxidation level of a given *N*,*N*′-coordinated *o*-phenylenediamine derivative such as *o*-phenylenediimide(2−), $(L^{PDI})^{2-}$, semiquinonate(1−), $(L^{ISQ})^{1-}$, or quinone, (L^{IBQ}) is clearly identifiable from the bond lengths, as shown in Figure 1. The average C_{arom}−NR distance of the *o*-phenylenediamine ring is indicative of a C═N double bond in M(L^{IBQ}) fragments at ∼1.30 Å or for a C−N bond order of ∼1.5 Å in M(L^{ISQ}) fragments at ∼1.35 Å, or for a C−N single bond in M(L^{PDI}) fragments at ∼1.39 Å.

Figure 3 displays the structure of a neutral molecule [$Ni^{II}(^3L^{ISQ})_2$] in crystals of **1**. Note that the molecule does not have crystallographically imposed symmetry. The C−C and C−N bond distances of both *N*,*N*′-coordinated ligands, $(^3L^{ISQ})^{1-\bullet}$, are identical within experimental error. The average C−NR bond length (Table 2) at 1.35 ± 0.01 Å is typical for the semiquinonate radical anion, $(^3L^{ISQ})^{1-}$, and

(12) Data sets of two crystals of **2** were measured at 100 K using Mo Kα radiation, but both refinements gave very poor results. We refrain from discussing detailed structural features of **2**, but the results clearly show that (a) the composition of the compound is in agreement with elemental analysis and other spectroscopic data and (b) the complex is not strictly planar since the coordination planes are significantly twisted by an angle of about 20°. Crystal data of **2**·MeCN: $C_{70}H_{95}N_5Pd$; fw = 1112.91; space group $P\bar{1}$, No. 2; $a = 10.2616(9)$ Å, $b = 16.973(2)$ Å, $c = 19.259(3)$ Å; $\alpha = 86.46(1)°$, $\beta = 78.66(1)°$, $\gamma = 74.38(1)°$; $V = 3167.3(7)$ Å^3; $Z = 2$; $T = 100(2)$ K.; $\rho_{calcd} = 1.16$ g cm^{-3}.

Table 2. Selected Bond Distances (Å) of Complexes

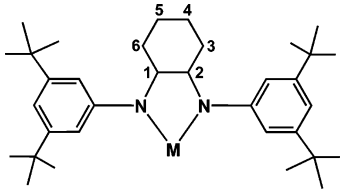

	1		
	ligand 1	ligand 2	**3**
M−N1	1.894(2)	(1.886(2))	1.920(5)
M−N2	1.901(2)	(1.905(2))	
N1−C1	1.350(3)	(1.337(3))	1.354(8)
N2−C2	1.349(3)	(1.351(3))	
C1−C2	1.451(3)	(1.447(3))	1.46(1)
C2−C3	1.417(4)	(1.418(4))	1.42(1)
C3−C4	1.361(4)	(1.368(4))	1.35(1)
C4−C5	1.413(4)	(1.414(4))	1.41(1)
C5−C6	1.364(4)	(1.357(4))	
C6−C1	1.422(4)	(1.417(4))	

consequently, the central nickel ion possesses a 2+ oxidation state and a high-spin d^8 electron configuration. Similarly, the average length of the two alternating short C═C bonds at 1.36 ± 0.01 Å of the *o*-phenylenediamine part in conjunction with four longer ones >1.39 Å are indicative of the semiquinonate oxidation level (quinoid-type distortion). It is quite remarkable and may serve as an internal standard for the high-quality X-ray determination that the six C−C distances of each of the 3,5-di-*tert*-butylphenyl substituents are equidistant at ∼1.392 ± 0.01 Å (aromatic phenyl rings).

The most interesting feature of the above structure of **1** is the observation of a pseudo-tetrahedral coordination sphere around the central Ni(II) ion: the two N−Ni−N angles of the two five-membered chelate rings Ni−N−C−C−N are 83.7° and 83.1° (±0.3°); the two planes of these five-membered rings form a dihedral angle of 85.4° (which is 90° in a regular tetrahedron and 0° in a square planar arrangement). The four different dihedral angles between the *N*-(3,5-di-*tert*-butylphenyl) rings and the five-membered chelate rings are irregular at 41.4° and 79.9° for one ligand

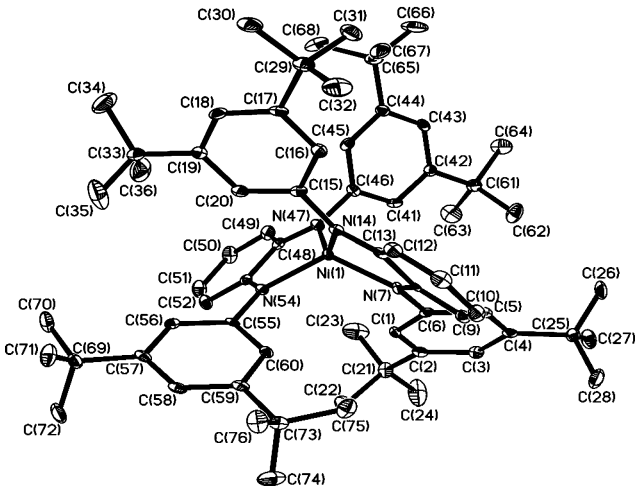

Figure 3. Structure of the neutral complex [$Ni^{II}(^3L^{ISQ})_2$] in crystals of **1**. The thermal ellipsoids of non-hydrogen atoms are drawn at the 50% probability level. Hydrogen atoms are omitted.

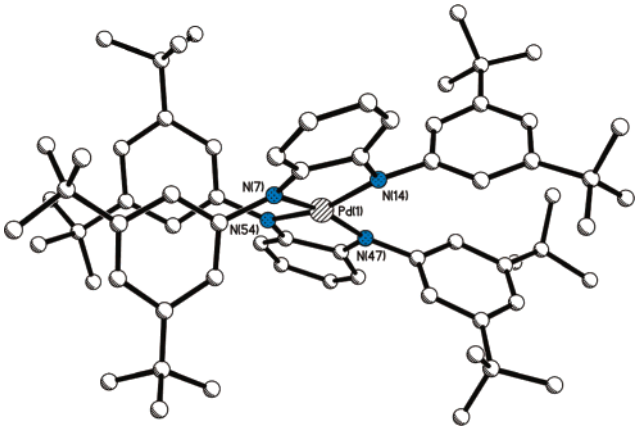

Figure 4. Ball-and-stick representation of the structure of the neutral complex $[Pd^{II}(^3L^{ISQ})_2]$ in crystals of **2**.

and at 36.7° and 26.2° for the other. It is interesting to note that the corresponding structures of complexes $[Ni^{II}(^1L^{ISQ})_2]$ [13] and $[Ni^{II}(^2L^{ISQ})_2]$ [2a] are both square planar. The average Ni−N bond distance in **1** is 1.896 Å and a little shorter at 1.842 Å in square planar $[Ni^{II}(^2L^{ISQ})_2]$.

Since two crystals of **2** selected for X-ray structure determinations proved to be of very low quality,[12] only the atom connectivity of the neutral molecule $[Pd(^3L)_2]$ has been established beyond reasonable doubt, as shown in Figure 4. It is clear that the molecule is not quite planar since the dihedral angle between the two five-membered Pd−N−C−C−N planes is 20.0°. Similar angles have been observed in a number of diamagnetic bis(chelate) palladium(II) complexes as, for example, in *trans*-bis[(phenylazo)acetaldoximato]palladium(II),[14] $[Pd(bpy)_2](NO_3)_2 \cdot H_2O$,[15] and $[Pd(1,10\text{-phenanthroline})_2](ClO_4)_2$.[16] Thus, for all practical purposes, the structure of the neutral molecule $[Pd(^3L^{ISQ})_2]$ is considered here to be almost planar. The structure of $[Pd^{II}(^2L^{ISQ})_2]$ is exactly square planar with a dihedral angle between the two ligand planes of 0°.[2a]

In contrast, the structure of the neutral molecule $[Co(^3L)_2]$ in crystals of **3** shown in Figure 5 possesses crystallographically imposed S_4 symmetry. The cobalt ion is in a tetrahedral environment of four nitrogen donor atoms. The dihedral angle between the two planar five-membered chelate rings is 90°. We also note that the average Co−N distance in tetrahedral **3** ($S = {}^3/_2$) is 1.920(5) Å but only 1.840 Å in square planar $[Co(^2L)_2]$ ($S = {}^1/_2$).[3]

The metrical details of the *N*,*N*′-coordinated *o*-phenylenediimide ligands in **3** apparently point to the semiquinonate(1−) oxidation level, $(^3L^{ISQ})^{1-\bullet}$: in particular, the average C−NR bond distance at 1.35 ± 0.02 Å and the quinoid-type distortion of the phenylene rings with two alternating short and four longer C−C bonds, respectively. On the other hand, it is noted that the equivalent isotropic displacement parameters for the C and N atoms in **3** are significantly larger than

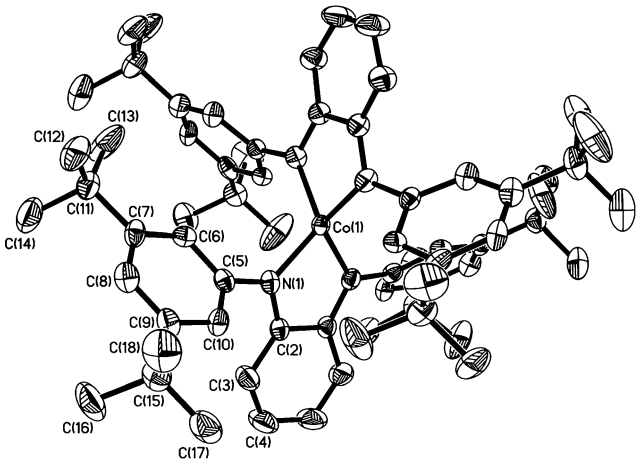

Figure 5. Structure of the neutral molecule $[Co(^3L)_2]$ in crystals of **3**. The thermal ellipsoids of the non-hydrogen atoms are drawn at the 50% probability level. Hydrogen atoms are omitted.

those of the corresponding atoms in **1**. For example, U_{eq} is $35(2) \times 10^{-3}$ Å^2 for the nitrogen atom in **3** but only on average 9×10^{-3} Å^2 for each nitrogen atom in **1**.

This could be taken as an indication for an unresolved static disorder involving one of the following structures A and B

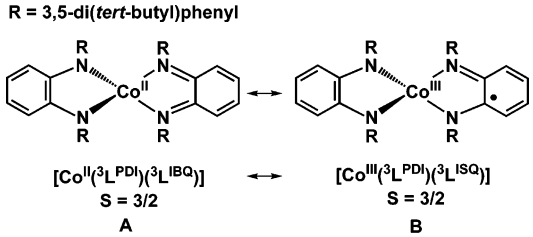

Formulae A,B

where the differing oxidation levels of the ligands are localized.

Superposition of two forms results in an apparent S_4 site symmetry, which would represent a static disorder and averaged C−C and C−N bond distances are observed only. Interestingly, the symmetric structure $[Co^{II}(^3L^{ISQ})_2]$ containing two genuine *o*-semiquinonate(1−) radicals, and a central cobalt(II) ion does not possess such large thermal parameters[3] but rather those as observed in **1**. In addition, as discussed below, a symmetric tetrahedral structure $[Co^{II}(^3L^{ISQ})_2]$ should possess an $S = {}^1/_2$ ground state since in tetrahedral $[Ni^{II}(^3L^{ISQ})_2]$ the two radical ligands couple strongly antiferromagnetically to a Ni^{II} ion with local $S_{Ni} = 1$, yielding the observed $S_t = 0$ ground state in **1** (see below). Therefore, a high-spin cobalt(II) ion with $S_{Co} = {}^3/_2$ would be coupled antiferromagnetically to two $(L^{ISQ})^{1-}$ radicals, yielding an $S_t = {}^1/_2$ ground state which is not observed. Note that square planar $[Co^{II}(^2L^{ISQ})_2]$ (or $[Co^{III}(^2L^{PDI})(^2L^{ISQ})]$) possesses an $S_t = {}^1/_2$ ground state.[3]

3. Electro- and Spectroelectrochemistry. The electrochemistry of **1**, **2**, and **3** in CH_2Cl_2 (0.10 M $[N(n\text{-}Bu)_4]PF_6$ supporting electrolyte) has been studied by cyclic voltammetry (cv) and coulometry at fixed potentials. The potentials given are referenced versus the ferrocenium/ferrocene (Fc^+/

(13) Swartz Hall, G.; Soderberg, R. H. *Inorg. Chem.* **1968**, *7*, 2300.
(14) Bandyopadhyay, D.; Bandyopadhyay, P.; Chakravorty, A.; Cotton, F. A.; Falvello, L. R. *Inorg. Chem.* **1984**, *23*, 1785.
(15) Hazell, A.; Simonsen, O.; Wernberg, O. *Acta Crystallogr.* **1986**, *C42*, 1707.
(16) Rund, J. V.; Hazell, A. C. *Acta Crystallogr.* **1980**, *B36*, 3103.

Table 3. Redox Potentials of Complexes in Volts vs Fc^+/Fc at 20 °C[a]

complex	$E^1_{1/2}$, V[b]	$E^2_{1/2}$, V[c]	$E^3_{1/2}$, V[d]	$E^4_{1/2}$, V[e]
1		−0.14 (2[e];r.)	−1.37(r.)	−1.79(q.r.)
$[Ni(^2L)_2]$[h]	0.21(r.)	−0.07(r.)	−1.21(r.)	−1.89(r.)
2	0.21(r.)	−0.23(r.)	−1.31(2[e];r.)	
$[Pd(^2L)_2]$[h]	0.24(r.)	−0.14(r.)	−1.22(r.)	−1.72(r.)
3	0.20(r.)	−0.14[f], −0.72[g]	−1.35(r.)	−1.85(r.)
$[Co(^2L)_2]$[i]		−0.50(r.)	−1.03(r.)	
$[Co(^1L)_2]$[j]		−0.32	−0.95	−1.98

[a] Conditions: CH_2Cl_2 solution (0.1 M $[N(n\text{-}Bu)_4]PF_6$). [b] 2+/1+ couple. [c] 1+/0 couple. [d] 0/1− couple. [e] 1−/2− couple. [f] Peak potential E_p^{ox}. [g] Peak potential E_p^{red}. [h] Reference 2a. [i] Reference 3. [j] Reference 1.

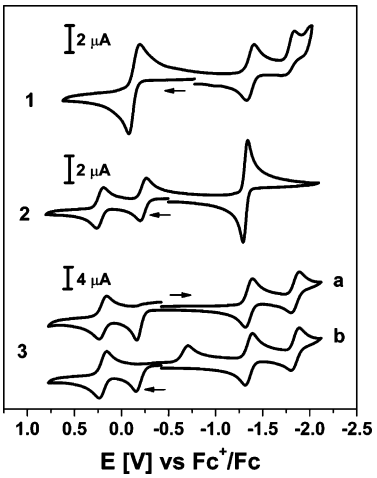

Figure 6. Cyclic voltammograms of **1**, **2**, and **3** in CH_2Cl_2 solution (0.10 M $[N(n\text{-}Bu)_4]PF_6$) at a glassy carbon working electrode at 20 °C. Potentials are referenced vs the Fc^+/Fc couple; scan rates 200 mV s^{-1}.

Fc) couple. The results are summarized in Table 3; Figure 6 shows the cv's of **1**, **2**, and **3**.

The cv of **1** displays a reversible, two-electron oxidation wave at −0.14 V, a reversible one-electron reduction wave at −1.37 V, and a quasi-reversible one-electron reduction wave at −1.79 V according to eq 1

$$[Ni^{II}(^3L^{IBQ})_2]^{2+} \underset{+2e}{\overset{-2e}{\rightleftharpoons}} [Ni^{II}(^3L^{ISQ})_2]^0 \underset{+e}{\overset{-e}{\rightleftharpoons}} [Ni^{II}(^3L^{PDI})(^3L^{ISQ})]^{1-} \underset{+e}{\overset{-e}{\rightleftharpoons}} [Ni^{II}(^3L^{PDI})_2]^{2-} \quad (1)$$

It is instructive to compare the electrochemical behavior of *tetrahedral* **1** with that reported for square planar $[Ni^{II}(^2L^{ISQ})_2]^2$ under identical conditions. The square planar complex undergoes two reversible one-electron oxidations and two one-electron reductions, eq 2, all of which are ligand-centered processes. Interestingly, the difference of half-wave potentials, $|\Delta E|$, for the couples $[NiL_2]^{0/1-}$ and $[NiL_2]^{1-/2-}$ of square planar and tetrahedral species are 680 and 420 mV, respectively. Similarly, for the couples $[NiL_2]^{0/1+}$ and $[NiL_2]^{1+/2+}$ the redox potential differences $|\Delta E|$ are 280 mV for the square

$$[Ni^{II}(^2L^{IBQ})_2]^{2+} \underset{+e}{\overset{-e}{\rightleftharpoons}} [Ni^{II}(^2L^{IBQ})(^2L^{ISQ})]^{+} \underset{+e}{\overset{-e}{\rightleftharpoons}} [Ni^{II}(^2L^{ISQ})_2]^0 \underset{-e}{\overset{+e}{\rightleftharpoons}} [Ni^{II}(^2L^{ISQ})(^2L^{PDI})]^{1-} \underset{+e}{\overset{-e}{\rightleftharpoons}} [Ni^{II}(^2L^{PDI})_2]^{2-} \quad (2)$$

planar case but ∼0 mV for the tetrahedral one. These data indicate that electronic coupling between the two ligands

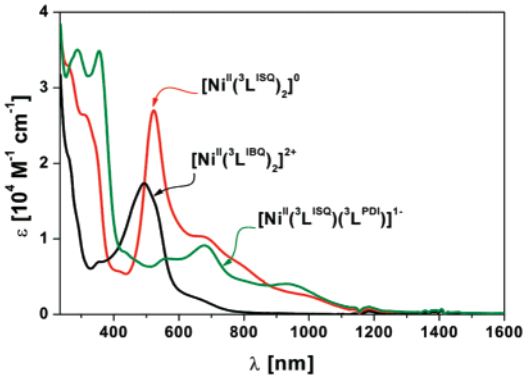

Figure 7. Electronic spectra of **1** (red), $\mathbf{1}^{2+}$ (black), and $\mathbf{1}^{1-}$ (green) in CH_2Cl_2 solution (0.10 M $[N(n\text{-}Bu)_4]PF_6$).

Table 4. Electronic Spectra of Complexes at 20 °C in CH_2Cl_2 Solution

complex	λ_{max}, nm (ϵ, 10^4 M^{-1} cm^{-1})
1	257sh(3.3), 307(2.65), 414(0.57), 523(2.70), 674(1.03), 800sh(0.64), 967sh(0.28)
$[\mathbf{1}]^{1-}$[a]	286(3.5), 355(3.48), 433sh(0.83), 565(0.74), 679(0.92), 934(0.40)
$[\mathbf{1}]^{2+}$[a]	259(2.1), 353(0.70), 492(2.73), 657sh(0.22)
2	261(3.7), 340(1.49), 421sh(0.30), 657(0.65), 710sh(0.65), 903(4.14)
$[\mathbf{2}]^{2+}$[a]	334(1.76), 489(1.28)
$[\mathbf{2}]^{1+}$[a]	311(2.73), 472(1.45), 563(0.8), 1177sh(0.21), 1733(2.54)
$[\mathbf{2}]^{2-}$[a]	295(4.01), 366(2.65)
3	263(2.9), 320sh(2.0), 490sh(1.16), 526(1.40), 725(0.72)
$[\mathbf{3}]^{1-}$[a]	268(2.8), 352(2.7), 488(0.6), 534(0.5)
$[\mathbf{3}]^{2-}$[a]	284(2.5), 358(3.0), 482sh(0.3), 562(0.1)
$[\mathbf{3}]^{+}$[a]	281sh(1.9), 502(1.0), 626sh(0.6), 871sh(0.1)
$[\mathbf{3}]^{2+}$[a]	493(1.4)

[a] Electrochemically generated in CH_2Cl_2 solution (0.1 M $[N(n\text{-}Bu)_4]PF_6$).

in the square planar ligand mixed-valence complexes $[Ni^{II}(L^{ISQ})(L^{IBQ})]^{1+}$ and $[Ni(L^{ISQ})(L^{PDI})]^{1-}$ is much more pronounced than in the corresponding tetrahedral analogues. It leads to the conclusion that the excess electron in the square planar monocationic and -anionic complexes is delocalized over both ligands (class III ligand mixed valency). On the other hand, in tetrahedral $[Ni^{II}(^3L^{PDI})(^3L^{ISQ})]^{1-}$, this may not be the case and a localized description is more appropriate. This has been reported recently in ref 17 for similar tetrahedral Ni(II) complexes.

Since it is possible to coulometrically generate the stable dication of **1** and its monoreduced form $[Ni^{II}(^3L^{PDI})(^3L^{ISQ})]^{1-}$ in CH_2Cl_2 solution containing 0.10 $[N(n\text{-}Bu)_4]PF_6$, we have recorded their electronic spectra which are shown in Figure 7 (Table 4). The doubly reduced form was too unstable on the time scale of the coulometry, and an electronic spectrum could not be recorded. It is then again instructive to compare these spectra with those reported for their square planar analogues.

The neutral tetrahedral complex $[Ni^{II}(^3L^{ISQ})_2]$ displays an intense absorption maximum at 523 nm ($\epsilon = 2.7 \times 10^4$ M^{-1} cm^{-1}) which is absent in the square planar species $[Ni^{II}(^2L^{ISQ})_2]$ for which a very intense ligand-to-ligand charge-transfer band is observed at 840 nm ($\epsilon = 4.0 \times 10^4$ M^{-1}

(17) Blanchard, S.; Neese, F.; Bothe, E.; Bill, E.; Weyhermüller, T.; Wieghardt, K. *Inorg. Chem.* **2005**, *44*, 3636.

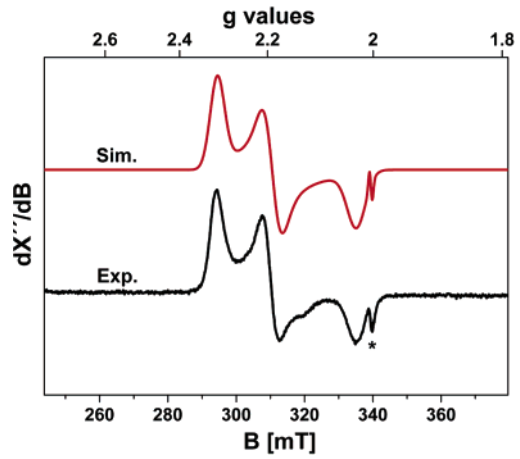

Figure 8. X-band EPR spectrum of a frozen CH_2Cl_2 solution (0.10 M $[N(n\text{-}Bu)_4]PF_6$) of the electrochemically generated monoanion $\mathbf{1}^{1-}$ at 10 K. (Conditions: frequency 9.520 GHz; power 2.0 μW; modulation 8 G). The asterisk denotes an organic radical impurity (~0.1%).

cm^{-1}) in the near-infrared (NIR) region which in turn is absent in **1**. Similarly, the electronic spectra of the presumably *tetrahedral* monoanion $[Ni^{II}(^3L^{ISQ})(^3L^{PDI})]^{1-}$ and of *square planar* $[Ni^{II}(^2L^{ISQ})(^2L^{PDI})]^{1-}$ differ significantly, although both possess an $S = {}^1/_2$ ground state. The square planar complex $[Ni(^2L^{ISQ})(^2L^{PDI})]^{1-}$ displays an intense intervalence charge-transfer band (IVCT) in the near-infrared (NIR) at 1120 nm ($\epsilon = 1.7 \times 10^4\ M^{-1}\ cm^{-1}$) which is absent in the spectrum of $[Ni^{II}(^3L^{ISQ})(^3L^{PDI})]^{1-}$ for which we consequently propose a tetrahedral structure with one localized $(^3L^{ISQ})^{1-\bullet}$ radical ligand and a $(^3L^{PDI})^{2-}$ ligand. We note that the tetrahedral monoanion does display two relatively intense absorption maxima at 679 and 934 nm (Table 4) which are tentatively assigned to LLCT bands involving class II behavior of the two ligands with localized oxidation levels $(^3L^{PDI})^{2-}$ and $(^3L^{ISQ})^{1-}$. The electronic structure of the planar monoanion is different: the unpaired electron is delocalized over both ligands (class III).

As shown in Figure 8, the X-band EPR spectrum of the monoanion of **1** displays a rhombic signal with relatively large *g* anisotropy: $g_x = 2.313$; $g_y = 2.190$; $g_z = 2.029$. A similar *g* anisotropy as a consequence of large spin−orbit coupling has been observed previously for similar tetrahedral, monoradical Ni(II) complexes.[17] Its electronic structure is then best described as a central paramagnetic Ni(II) ion ($S_{Ni} = 1$) coupled antiferromagnetically to a single ligand radical ($S_{rad} = {}^1/_2$), yielding the observed $S_t = {}^1/_2$ ground state. As noted above, the tetrahedral monoanion displays two relatively intense absorption maxima at 679 and 934 nm (Table 4) which are tentatively assigned to LLCT bands involving class II behavior of the two ligands with localized oxidation levels $(^3L^{PDI})^{2-}$ and $(^3L^{ISQ})^{1-}$. In contrast, the EPR spectrum of square planar $[Ni^{II}(^2L^{PDI})(^2L^{ISQ})]^{1-}$ displays[2] a rhombic signal with a significantly smaller *g* anisotropy: $g_x = 1.994$; $g_y = 2.007$; $g_z = 2.100$ indicative of a delocalized ligand radical and a diamagnetic Ni(II) center.

The electronic spectrum of the dianion of tetrahedral **1** is expected not to exhibit charge-transfer bands in the visible or NIR, in analogy to square planar dianion $[Ni^{II}(^2L^{PDI})_2]^{2-}$ [2] and complex **2**. Note that square planar $[Ni^{II}(^2L^{PDI})_2]^{2-}$ is

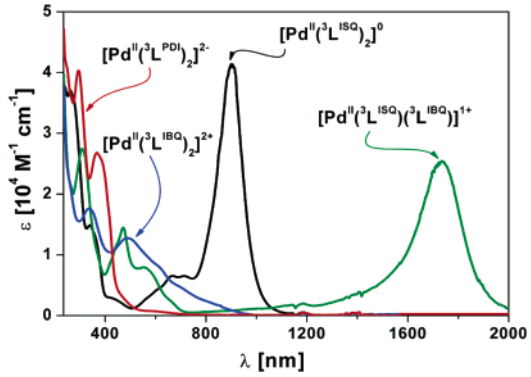

Figure 9. Electronic spectra of **2** and electrochemically generated $\mathbf{2}^{2+}$; $\mathbf{2}^{1+}$; $\mathbf{2}^{2-}$ in CH_2Cl_2 solution (0.10 M $[N(n\text{-}Bu)_4]PF_6$).

diamagnetic,[2] whereas for a tetrahedral $[Ni^{II}(^3L^{PDI})_2]^{2-}$ complex, an $S = 1$ ground state is expected. Similarly, square planar $[Ni^{II}(^2L^{IBQ})_2]^{2+}$ is diamagnetic but tetrahedral $[Ni^{II}(^3L^{IBQ})_2]^{2+}$ is expected to be again paramagnetic ($S = 1$).

The cv of **2** displays three reversible electron-transfer waves (Figure 6; Table 3): two successive one-electron oxidations yielding a mono- and a dication and a reversible two-electron reduction step yielding the dianion, as depicted in eq 3. All observed redox processes are considered to be ligand centered.[2,3,17]

$$[Pd^{II}(^3L^{IBQ})_2]^{2+} \underset{+e}{\overset{-e}{\rightleftharpoons}} [Pd^{II}(^3L^{IBQ})(^3L^{ISQ})]^{+} \underset{+e}{\overset{-e}{\rightleftharpoons}} [Pd^{II}(^3L^{ISQ})_2]^{0} \underset{+2e}{\overset{-2e}{\rightleftharpoons}} [Pd^{II}(^3L^{PDI})_2]^{2-} \quad (3)$$

Figure 9 and Table 4 show the electronic spectra of the above species. It is interesting to note that the redox potentials $E^1_{1/2}$ and $E^2_{1/2}$ for **2** and $[Pd^{II}(^2L^{ISQ})_2]^0$ are very similar. $E^3_{1/2}$ corresponds to a one-electron reduction for the latter and a two-electron process for the former yielding a mono- and a dianion, respectively. This is good evidence that **2**, its oxidized species, and its reduced species behave as square planar complexes such as those of $[Pd^{II}(^2L^{ISQ})_2]$ reported earlier.[2] This notion is further corroborated by the observation that the X-band EPR spectrum of the monocation $[Pd^{II}(^3L^{IBQ})(^3L^{ISQ})]^{1+}$ recorded at 10 K in frozen CH_2Cl_2 displays a broad, nearly isotropic signal at $g_1 = 2.0052$, $g_2 = 2.0032$, $g_3 = 1.9982$; $g_{iso} = 2.0022$ with only very small *g* anisotropy and no Pd hyperfine coupling. The EPR spectrum of $[Pd^{II}(^2L^{IBQ})(^2L^{ISQ})]^{1+}$ is similar.[2] These results indicate the presence of the same delocalized ligand-centered radical $[Pd^{II}(L^{IBQ})(L^{ISQ})]^{1+} \leftrightarrow [Pd^{II}(L^{ISQ})(L^{IBQ})]^{1+}$ in both complexes containing *N*-phenyl- and *N*,*N*′-diphenyl-substituted ligands.

Furthermore, both paramagnetic monocations $[Pd^{II}(^2L^{IBQ})(^2L^{ISQ})]^{1+}$ and $[Pd^{II}(^3L^{IBQ})(^3L^{ISQ})]^{1+}$ exhibit an intense IVCT band in the NIR region at 1617 ($2.6 \times 10^4\ M^{-1}\ cm^{-1}$) and 1733 nm ($2.5 \times 10^4\ M^{-1}\ cm^{-1}$), respectively. Similarly, both the neutral complexes **2** and $[Pd^{II}(^2L^{ISQ})_2]$ display an intense LLCT band at 903 ($4.1 \times 10^4\ M^{-1}\ cm^{-1}$) and 840 nm ($4.1 \times 10^4\ M^{-1}\ cm^{-1}$), respectively. In summary, the spectroscopic data reported here for almost planar **2** and their oxidized and reduced forms are very similar to those reported

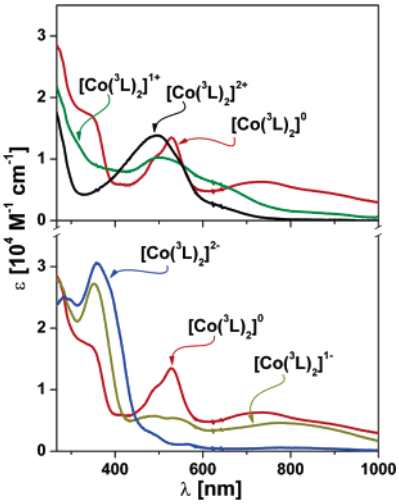

Figure 10. Electronic spectra of **3** (red), $\mathbf{3}^{1+}$ (green), $\mathbf{3}^{2+}$ (black); $\mathbf{3}^{2-}$ (blue), $\mathbf{3}^{1-}$ (yellow-green) in CH_2Cl_2 solution (0.10 M $[N(n\text{-}Bu)_4]PF_6$) at 20 °C.

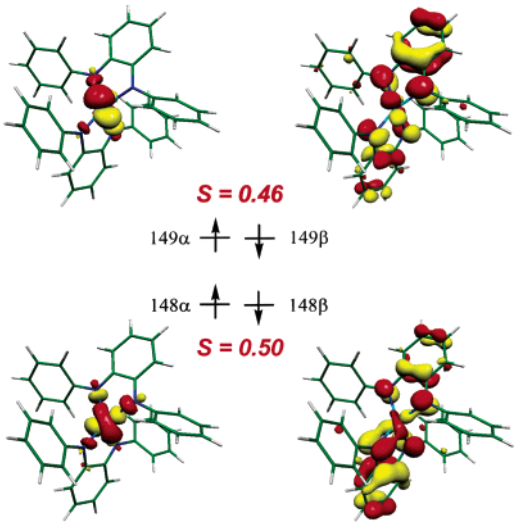

Figure 11. Qualitative MO diagram of the corresponding orbitals of magnetic pairs of **1** as derived from the broken symmetry DFT calculations (B3LYP).

for the strictly planar analogue containing the less-bulky *N*-phenyl *o*-phenylenediamine derivatives.

The cv of the cobalt complex **3** displays four one-electron transfer waves: two successive reversible reductions and two oxidation steps (Figure 6) of which the second oxidation is reversible too. This first oxidation step is irreversible in character, the anodic and cathodic waves are separated by 0.58 V. Such large peak separation can be caused by slow heterogeneous electron transfer kinetics or by a chemical reaction following oxidation. The peak positions do not depend strongly on the scan rate, which argues against the former mechanism, which, however, is not fully ruled out. The latter mechanism (chemical reaction) would yield a redox potential around −0.1 V, which is very close to redox potentials of **1** and **2**. Thus, an electron-transfer series $[Co(^2L)_2]^z$ consisting of five species with $z = 2+, 1+, 0, 1-, 2-$ is established for **3**. It is noted that a chemical reaction, if it was responsible for the potential shift of the cathodic wave, must be reversible. Otherwise, the second oxidation step to the dication would hardly be observed at +0.2 V, which is very similar to those of **2** and the square planar complexes $[Ni^{II}(^2L^{ISQ})_2]$ and $[Pd^{II}(^2L^{ISQ})_2]$, in which the following reactions are absent.[2] Spectroelectrochemical measurements on the respective electrochemically generated species reveal their electronic spectra, which are shown in Figure 10 (Table 4). Since the molecular and electronic structures of the oxidized and reduced species of **3** are at present not known, we refrain from commenting on their electronic structures. The electronic spectrum of tetrahedral **3** is quite different from that reported in ref 3 in Figure 11 for square planar $[Co(^2L^{ISQ})_2]$. The latter displays an intense LLCT band at 1230 nm (0.4×10^4 M^{-1} cm^{-1}) which is absent in the spectrum of **3**. Thus, the electronic structures of both neutral species are different.

4. DFT Calculations. a. Optimized Geometries for 1. In this section, a detailed picture of the molecular and electronic structure of the neutral complex **1** will be developed. For this purpose, we have used a truncated version of complex **1** where the eight *tert*-butyl groups have been removed and substituted by eight hydrogen atoms. Assuming that tetrahedral **1** features a high-spin Ni(II) ion and two ligand radicals, we optimized the ground-state geometry for (a) a closed shell $S = 0$, (b) a high-spin, open-shell $S = 2$, and (c) a BS $M_S = 0$ state for truncated **1**.

Table 5. Calculated and Experimental Bond Distances in Å

	B3LYP, BS	B3LYP, closed shell	B3LYP, high spin	exptl
Ni(1)−N(7)	1.976	1.893	1.997	1.894(2)
Ni(1)−N(14)	1.980	1.893	2.028	1.901(2)
Ni(1)−N(47)	1.973	1.893	1.998	1.886(2)
Ni(1)−N(54)	1.986	1.894	2.027	1.905(2)
N(7)−C(8)	1.345	1.356	1.346	1.350(3)
N(14)−C(13)	1.348	1.356	1.347	1.349(3)
C(8)−C(9)	1.429	1.424	1.427	1.422(4)
C(8)−C(13)	1.464	1.445	1.470	1.451(3)
C(9)−C(10)	1.379	1.383	1.380	1.364(4)
C(10)−C(11)	1.422	1.418	1.421	1.413(4)
C(11)−C(12)	1.380	1.383	1.380	1.361(4)
C(12)−C(13)	1.428	1.424	1.429	1.417(4)
N(47)−C(48)	1.347	1.356	1.349	1.337(3)
N(54)−C(53)	1.345	1.356	1.347	1.351(3)
C(48)−C(49)	1.428	1.424	1.426	1.417(4)
C(48)−C(53)	1.465	1.445	1.468	1.447(3)
C(49)−C(50)	1.379	1.383	1.381	1.357(4)
C(50)−C(51)	1.423	1.416	1.420	1.414(4)
C(51)−C(52)	1.379	1.383	1.380	1.368(4)
C(52)−C(53)	1.430	1.424	1.429	1.418(4)

For all three cases, stationary states on the potential energy surface were located. The closed-shell solution is 8 kcal mol^{-1} higher in energy than the BS solution, and the $S = 2$ configuration is even 9 kcal mol^{-1} higher in energy. Thus the BS solution involving a high-spin Ni(II) ion antiferromagnetically coupled to two ligand π-radical monoanions, $(^3L^{ISQ})^{1-}$, is the preferred one. The calculated bond distances of the BS solution within the ligands are in acceptable agreement with experiment (Table 5) and support the presence of two $(^3L^{ISQ})^{1-}$ π radicals. The average Ni−N distance at 1.979 Å is overestimated by 0.08 Å; a result which is typical for the B3LYP functional.[17] Interestingly, the BS calculated dihedral angle between the two metallacycles in **1** at 86° is in excellent agreement with experiment (85.4°). This angle is calculated to be only 40° in the closed-

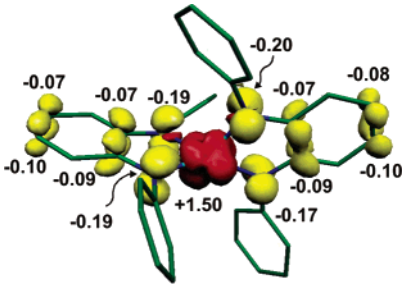

Figure 12. Spin density plot of **1** as derived from BS DFT calculations together with values of the spin density of the Mulliken spin population analysis. Hydrogen atoms are omitted for clarity.

shell $S = 0$ calculation (approaching a square planar structure). The high-spin model features a geometry very similar to that of the BS solution with slightly longer Ni−N disctances and a dihedral angle of 88°.

b. Electronic Structure of 1. A qualitative bonding scheme derived from the spin-unrestricted BS calculation of **1** is shown in Figure 11. Five orbitals which are predominantly of metal d character are identified. Three of these orbitals (not shown) are found in the spin-up and the spin-down manifolds; they are doubly occupied. The other two nickel-based orbitals originate from the t_2 set and occur only in the spin-up manifold. These two orbitals are thus singly occupied with parallel spins. This orbital occupation pattern defines a high-spin Ni(II) configuration ($S_{Ni} = 1$) at the metal center. In addition to these two metal-centered orbitals, two ligand-centered orbitals are identified in the spin-down manifold which are not populated in the spin-up manifold, thus leading to the observed overall $M_S = 0$ BS state. These orbitals correspond to two symmetry-adapted combinations of the SOMO of the two ligand radicals. Thus, the basic electronic structure description of **1** features a high-spin Ni(II) ion which is strongly antiferromagnetically coupled to two ligand-centered π radicals, as has been proposed by the authors of refs 17 and 18 for similar complexes. It is the antiferromagnetic ligand-to-metal coupling which dominates in **1**. In contrast, in the square planar analogues $[Ni^{II}(^{1,2}L^{ISQ})_2]$[2,3] a very strong ligand-to-ligand antiferromagnetic coupling prevails. For nearly square planar **2**, we propose this latter coupling scheme. As discussed previously,[2,3] this strong intramolecular antiferromagnetic coupling is evidenced by an intense ($\epsilon > 10^4$ L mol^{-1} cm^{-1}) absorption band in the NIR region; the position and intensity of which is directly correlated with this antiferromagnetic coupling in the ground state.[2b] In tetrahedral **1**, such ligand-to-ligand coupling does not exist since the two planes of the coordinated radical ligands are nearly orthogonal to each other.

As pointed out previously,[2,19] the spin density arising from BS SCF (DF or HF) calculations is unphysical. Nevertheless, it is quite suggestive of the physical situation at hand. The spin density plot shown in Figure 12 nicely shows the antiparallel spin alignment between the high-spin Ni(II) (positive spin density in red) and the radical ligands (negative spin density in yellow). An approximate breakdown of the spin density into atomic contributions via a spin population analysis supports the presence of two unpaired electrons at the nickel ion with a positive spin and two unpaired electrons with a negative spin localized on the two ligand π radicals.

The corresponding orbital transformation[20] can be used to visualize the overlapping magnetic pairs of the system.[2,17,19,21] The spin−orbitals obtained from single-point unrestricted calculations were transformed in such a way that for each spin-up orbital there exists at most one spin-down partner that has nonzero spatial overlap. Values of S close to 1 indicate a standard doubly occupied MO with little spin-polarization, whereas $S \ll 1$ is the signature of nonorthogonal magnetic orbital pairs. For **1**, two such magnetically interacting pairs which interact via a π pathway have been identified. Each of these pairs consists of one metal orbital and the corresponding ligand radical orbital. The mutual overlap between those two orbitals are 0.46 and 0.50, as shown in Figure 11. This indicates fairly strong antiferromagnetic interactions between the two metal and two ligand radicals.

To determine the exchange coupling constant, we examined the high-spin and BS energies together with the corresponding spin-expectation values $\langle S^2 \rangle$ according to the Yamaguchi approach, eqs 1 and 2.[22] The meaning of $\langle S^2 \rangle$ has been described previously in refs 2b and 17.

$$H_{HDvV} = -2J\,\hat{S}_A\hat{S}_B \tag{1}$$

$$J = \frac{E_{HS} - E_{BS}}{\langle S^2 \rangle_{HS} - \langle S^2 \rangle_{BS}} \tag{2}$$

In this manner, J was estimated to be -946 cm^{-1} for **1**. This calculated large value is in accord with the experimental finding that the complex possesses a singlet ground state up to room temperature with no indication of thermal population of higher spin states. However, since J is too large to be verified experimentally, the accuracy of this calculation cannot be assessed.

Conclusions

In this study, it has been demonstrated experimentally and by DFT calculations that the electronic structure of the neutral tetrahedral complex **1** is best described as a molecule containing a high-spin nickel(II) central ion with an intrinsic spin state $S_{Ni} = 1$ which is *N*,*N*′-coordinated to two ligand π radicals ($S_{rad} = {}^1/_2$), $(^3L^{ISQ})^{1-\bullet}$. The latter are intramolecularly antiferromagnetically coupled to the nickel(II) ion, yielding an $S_t = 0$ ground state. In contrast, as shown previously,[2] the diamagnetic, square planar analogue

(18) (a) Whalen, A. K.; Bhattacharya, S.; Pierpont, C. G. *Inorg. Chem.* **1994**, *33*, 347. (b) Bencini, A.; Carbonera, C.; Dei, A.; Vaz, M. G. F. *Dalton Trans.* **2003**, 1701. (c) Remenyi, C.; Kaupp, M. *J. Am. Chem. Soc.* **2005**, *127*, 11399. (d) Han, W. G.; Liu, T. Q.; Lovell, T.; Noodleman, L. *J. Am. Chem. Soc.* **2005**, *127*, 15778.
(19) Neese, F. *J. Phys. Chem. Solids* **2004**, *65*, 781.
(20) (a) Amos, A. T.; Hall, G. G. *Proc. R. Soc., Ser. A* **1961**, *263*, 483. (b) King, H. F.; Stanton, R. E.; Kim, H.; Wyatt, R. E.; Parr, R. G. *J. Chem. Phys.* **1967**, *47*, 1936.
(21) Ghosh, P.; Bill, E.; Weyhermüller, T.; Neese, F.; Wieghardt, K. *J. Am. Chem. Soc.* **2003**, *125*, 1293.
(22) a) Yamaguchi, K.; Takahara, Y.; Fueno, T. In *Applied Quantum Chemistry*; Smith, V. H., Ed.; Reidel: Dordrecht, 1986; p 155. (b) Soda, T.; Kitagawa, Y.; Ouishi, T.; Takano, Y.; Shigeta, Y.; Nagao, H.; Yoshioka, Y.; Yamaguchi, K. *Chem. Phys. Lett.* **2000**, *319*, 223.

$[Ni^{II}(^2L^{ISQ})_2]$ consists of a nickel(II) ion with an intrinsic $S_{Ni} = 0$ spin state and two ligand π radicals $(^2L^{ISQ})^{1-\bullet}$, which are intramolecularly antiferromagnetically coupled, affording the observed $S_t = 0$ ground state. The latter molecule is therefore a singlet diradical.[2] It is remarkable that the square planar species displays an intense LLCT band at 840 nm (4×10^4 M^{-1} cm^{-1}) which is absent in **1**.

The electronic structures of the one-electron transfer reduced monoanions, namely the presumably tetrahedral $[Ni^{II}(^3L^{ISQ})(^3L^{PDI})]^{1-}$ and the square planar $[Ni^{II}(^2L^{ISQ})(^2L^{PDI})]^{1-}$, differ also significantly despite the fact that both possess an $S_t = {}^1/_2$ ground state. It has been shown previously[2] that the square planar monoanion displays an intense IVCT band in the NIR at 1120 nm (1.7×10^4 M^{-1} cm^{-1}) which is absent in $\mathbf{1}^-$. The excess electron has been shown to be delocalized over both ligands (class III ligand mixed valency). Its rhombic EPR signal displays a moderate *g* anisotropy (1.994; 2.007; 2.100). Thus, the electronic structure of this square planar anion consists of a diamagnetic Ni(II) ion, a $(^2L^{ISQ})^{1-\bullet}$ π radical, and a $(^2L^{PDI})^{2-}$ ligand (delocalized). Consequently, the EPR signal has very little metal character. In contrast, the EPR spectrum of presumably tetrahedral $\mathbf{1}^-$ displays a significantly larger *g* anisotropy (2.029, 2.190, 2.313). This and the absence of a IVCT band in the NIR indicate that the electronic structure of $\mathbf{1}^-$ with $S_t = {}^1/_2$ is to be described as consisting of a high-spin nickel(II) ion ($S_{Ni} = 1$) coupled antiferromagnetically to a single, a localized $(^3L^{ISQ})^{1-\bullet}$ π radical, and a localized closed-shell dianion $(^3L^{PDI})^{2-}$. Consequently, the EPR signal exhibits significant metal character.

Although experimental data are not available, we propose that the dication $[Ni^{II}(^3L^{IBQ})_2]^{2+}$, if tetrahedral, possesses an $S_t = 1$ ground state whereas the square planar dication $[Ni^{II}(^2L^{IBQ})_2]^{2+}$ has an $S_t = 0$ ground state. Similarly, the tetrahedral dianion $[Ni^{II}(^3L^{PDI})_2]^{2-}$ should be paramagnetic ($S_t = 1$) whereas square planar $[Ni^{II}(^2L^{PDI})_2]$ is diamagnetic.

Interestingly, the square planar monocation $[Ni^{II}(^2L^{IBQ})(^2L^{ISQ})]^{1+}$ is electrochemically accessible[2] whereas tetrahedral $[Ni^{II}(^3L^{IBQ})(^3L^{ISQ})]^{1+}$ is not. The electronic spectrum of the former displays again an intense IVCT band at 1513 nm (0.9×10^4 M^{-1} cm^{-1}), indicating the delocalized nature of the ligand mixed valency.

The electronic structures of tetrahedral **3** ($S_t = {}^3/_2$) and of its square planar analogue $[Co(^2L)_2]$ ($S_t = {}^1/_2$) are more difficult to describe. DFT and correlated ab initio calculations on the latter species have shown that it is not possible to assign spectroscopic oxidation states describing a d^6 (Co^{III}) or d^7 (Co^{II}) electron configuration because the energies of ligand orbitals and metal d orbitals are very similar.[3] In particular, the out-of-plane orbital $2b_{2g}$ has almost equal contributions from the Co $3d_{xz}$ and the b_{2g} ligand fragment orbital. The electronic structure of $[Co(^2L)_2]$ ($S_t = {}^1/_2$) has been denoted by the following three resonance structures:[3]

$$[Co^{III}(^2L^{ISQ})(^2L^{PDI})] \leftrightarrow [Co^{III}(^2L^{PDI})(^2L^{ISQ})] \leftrightarrow [Co^{II}(^2L^{ISQ})_2]$$

A d^6 configuration (Co^{III}) in a square planar arrangement gives rise to an intrinsic $S_{Co} = 1$ spin state which is coupled antiferromagnetically to a single ligand radical. The observed EPR signal possesses, consequently, a large metal character and a significant *g* anisotropy (1.9906; 2.0508; 2.8100).[3] For tetrahedral **3**, the following resonance structures might explain the $S_t = {}^3/_2$ ground state:

$$[Co^{III}(^3L^{PDI})(^3L^{ISQ})] \leftrightarrow [Co^{II}(^3L^{IBQ})(^3L^{PDI})]$$

where a d^6 configuration (Co^{III}) in a tetrahedral ligand field gives rise to an $S_{Co} = 2$ state, which is antiferromagnetically coupled to a single (localized) $(^3L^{ISQ})^{1-\bullet}$ π radical affording the $S_t = {}^3/_2$, or alternatively, where a d^7 configuration (Co^{II}) in a tetrahedral ligand field gives rise to an $S_{Co} = {}^3/_2$ ground state (note that both ligands are now of the closed-shell type).

Acknowledgment. We thank the Fonds der Chemischen Industrie for financial support.

Supporting Information Available: X-ray crystallographic files for compounds **1** and **3**. This material is available free of charge via the Internet at http://pubs.acs.org.

IC060242L